

Letter

Observation of bound excited states in ^{15}B

M. Stanoiu¹, M. Belleguic¹, Zs. Dombrádi^{2,a}, D. Sohler², F. Azaiez¹, B.A. Brown³, M.J. Lopez-Jimenez⁴, M.G. Saint-Laurent⁴, O. Sorlin¹, Yu.-E. Penionzhkevich⁵, N.L. Achouri⁶, J.C. Angélique⁶, C. Borcea⁷, C. Bourgeois¹, J.M. Daugas⁴, F. De Oliveira-Santos⁴, Z. Dlouhy⁸, C. Donzaud¹, J. Duprat¹, S. Grévy⁶, D. Guillemaud-Mueller¹, S. Leenhardt¹, M. Lewitowicz⁴, S.M. Lukyanov⁵, W. Mittig⁴, M.G. Porquet⁹, F. Pougheon¹, P. Roussel-Chomaz⁴, H. Savajols⁴, Y. Sobolev⁵, C. Stodel⁴, and J. Timár²

¹ Institut de Physique Nucléaire, IN2P3-CNRS, F-91406 Orsay Cedex, France

² Institute of Nuclear Research, H-4001 Debrecen, Pf. 51, Hungary

³ NSCL, Michigan State University, East Lansing, MI 48824-1321, USA

⁴ GANIL, B.P. 55027, F-14076 Caen Cedex 5, France

⁵ FLNR, JINR, 141980 Dubna, Moscow region, Russia

⁶ Laboratoire de Physique Corpusculaire, F-14050 Caen Cedex, France

⁷ IFIN-HH, P.O. Box MG-6, 76900 Bucarest-Magurele, Romania

⁸ Nuclear Physics Institute, AS CR, CZ-25068, Rez, Czech Republic

⁹ CSNSM, IN2P3-CNRS and Université Paris-Sud, F-91405 Orsay Campus, France

Received: 4 May 2004 / Revised version: 2 September 2004 /

Published online: 19 October 2004 – © Società Italiana di Fisica / Springer-Verlag 2004

Communicated by J. Äystö

Abstract. The structure of the $A/Z = 3$ nucleus ^{15}B has been investigated using the in-beam γ -spectroscopy technique with a fragmentation reaction of a ^{36}S beam on a ^9Be target at $77.5 \text{ MeV} \cdot A$. The fragments were identified and selected by their energy loss and time of flight using the SPEG spectrograph. γ -ray energies and intensities have been measured in coincidence with the projectile-like fragments. From this information as well as from the $\gamma\gamma$ -coincidence relationships a level scheme is proposed for ^{15}B up to the neutron separation energy. The experimental results have been interpreted using shell model calculations in the psd valence space. Effects of the weakly bound nature of the valence neutrons have been observed.

PACS. 25.70.Mn Projectile and target fragmentation – 23.20.Lv γ transitions and level energies – 27.20.+n $6 \leq A \leq 19$ – 21.60.Cs Shell model

The structure of very neutron-rich nuclei came into the focus of interest, because some novel structural effects are expected in some of these exotic nuclei. Among others, the structure of neutron-rich boron isotopes attracted attention in the last decade mainly because the odd-proton boron nuclei represent weakly bound systems. In the early experimental studies of heavy boron nuclei, their ground-state properties were primarily investigated. By measuring an increased interaction cross-section in relativistic nuclear reactions [1], the existence of a neutron skin or halo could be demonstrated also in the ^{15}B isotope with $A/Z = 3$. The increased neutron radius is considered as a typical consequence of the weak binding and of the large neutron excess. These features, typical for drip line nuclei, may have consequences also on other properties of nuclei, like the energies of the excited states.

Concerning the excited states in ^{15}B , several unbound states could be revealed by use of multi-nucleon transfer reactions [2]. According to preliminary reports, γ -rays indicating the existence of bound excited states were observed in ^{15}B from in-beam γ -ray spectroscopy with fragmentation reactions [3, 4].

Theoretical predictions on the structure of neutron-rich boron nuclei are different from one approach to another. For instance, the antisymmetrized molecular-dynamics model (AMD) [5] suggests a transitional, deformed structure for ^{15}B , while shell model calculations predict a much smaller value of the moment of inertia which can be associated with a more moderate deformation [6, 7].

We have developed the method of in-beam γ -ray spectroscopy of projectile fragmentation reaction in GANIL in order to study the structure of neutron-rich nuclei [8, 9].

^a e-mail: domb@atomki.hu

This method has been applied to investigate several nuclei in the region of the $N = 28$ shell closure like the $^{45,46}\text{Ar}$ [10], $^{43,45}\text{Cl}$ [11], and $^{40,42,44}\text{S}$ nuclei [12] via fragmentation of the ^{48}Ca beam. The fragmentation of the ^{36}S beam has been applied to obtain information on the sub-shell closures at $N = 14, 16$ [13]. In the same set of data we could extract information on the bound excited states of $^{14,15}\text{B}$. In the present paper we report on the results obtained on the structure of these nuclei.

A $^{36}\text{S}^{16+}$ beam of 77.5 MeV \cdot A energy and 15 enA intensity was fragmented on a ^9Be target of 2.77 mg/cm² thickness. The emerging ^{15}B fragments were detected by the SPEG magnetic spectrometer. Ionization and drift chambers, as well as a plastic scintillator were placed at its focal plane, which provided data on the energy loss, total energy, and time of flight of the fragments. The fragments were identified by use of a standard ΔE -time-of-flight method. The time of flight was taken from the timing signals in the plastic scintillator with respect to the cyclotron radio frequency. It was corrected from the position of the fragments in the focal plane of the SPEG spectrometer to obtain a better time resolution and subsequently a better identification of the nuclei. Altogether 43 different isotopes have been identified in the experiment. We have collected $6 \cdot 10^5$ ^{14}B and $9 \cdot 10^4$ ^{15}B nuclei in the spectrograph.

The γ -rays emitted in flight by the excited fragments were detected by the 74 BaF₂ detectors of the “Chateau de crystal” and 4 hyper pure Ge detectors of 70% relative efficiency. The BaF₂ crystals were mounted symmetrically above and below the target at a mean distance of 21 cm covering about $\sim 80\%$ of the total solid angle. The spectra obtained in the BaF₂ detectors situated at forward angles (smaller than $\sim 40^\circ$) were found to contain a large background due to fast neutrons emitted in break-up reactions. These spectra were not used in the analysis in order to improve sensitivity by raising the signal-to-noise ratio in the γ -ray spectra. As the detectors were closely packed, the γ -rays could easily scatter from one to another. To decrease the background caused by the scattered γ -rays we used the array in anti-Compton mode, by rejecting all the events where at least 2 neighboring detectors have fired at the same time. Due to the relatively high efficiency of the BaF₂ array of about 20% at 1.3 MeV, for the stronger transitions, $\gamma\gamma$ -coincidence techniques could be exploited. The Ge detectors were placed at about 16 cm from the target at the most backward angles of 162° and 145° with respect to the beam direction. The total efficiency of the Ge spectrometer was $\sim 0.12\%$ at about 1300 keV.

The γ -ray spectra were corrected for the Doppler shift caused by the large fragment velocity ($v/c = 0.34$). For a raw Doppler correction the beam speed and the geometric detector positions were used. Two corrections were applied to this transformation: first, a mass-dependent correction was used, which takes into account that the average speed of the fragments depends on the number of nucleons removed. According to the reaction theory, the energy transfer has a linear mass dependence. To determine the parameters of the linear function, we fitted a

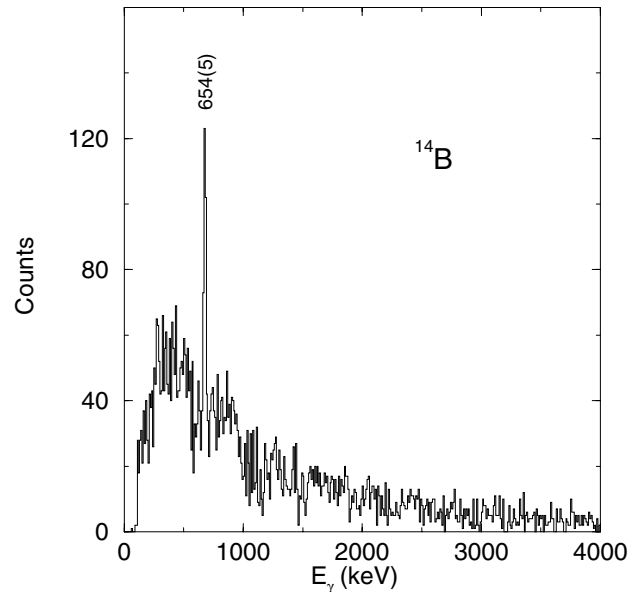


Fig. 1. The γ -ray spectrum of ^{14}B from fragmentation of a ^{36}S beam obtained by use of Ge detectors is shown.

line to the energies of γ -rays known precisely from previous studies. Second, to compensate for the statistical uncertainty in the speed of a given isotope arising from the statistical nature of energy transfer in the fragmentation reaction, the information on the momenta of the fragments provided by the SPEG spectrograph was applied similarly to the correction used in the time-of-flight method. Using these corrections, we applied a slightly mass-dependent internal energy calibration and in this way corrected for the systematic errors caused by different geometrical uncertainties. As a result, the energies of 30 known lines in the 200–3700 keV energy region of 17 different isotopes in the $A = 10$ –32 mass region were reproduced with less than 4 keV RMS deviation by use of the Ge detectors. Therefore, a 4 keV systematic error was assigned to their energy determination. For the BaF₂ array, less peaks could be used for internal calibration due to the lower energy resolution. The energy of 14 transitions in the 900–3700 keV energy region has been reproduced within a 26 keV RMS deviation for the BaF₂ setup.

The quality of the Doppler correction influenced also the resolution of the spectrometers especially for the BaF₂ array, where spectra from a wide angular range were added. After the above corrections a full width at a half-maximum (FWHM) of ~ 38 keV was obtained at the γ -ray energy of ~ 1500 keV in the Ge detectors and a 12% energy resolution was achieved with the BaF₂ array.

As a typical γ spectrum, we show the Ge spectrum of ^{14}B in fig. 1. In the spectrum we can see a single γ line at 654 ± 5 keV. The energy of the first-excited state in this nucleus was adopted as 740 ± 40 keV [14]. In the γ spectrum there is no sign of a transition corresponding to the decay of a state with that energy. On the other hand, the two energies slightly overlap at the 2σ confidence level,

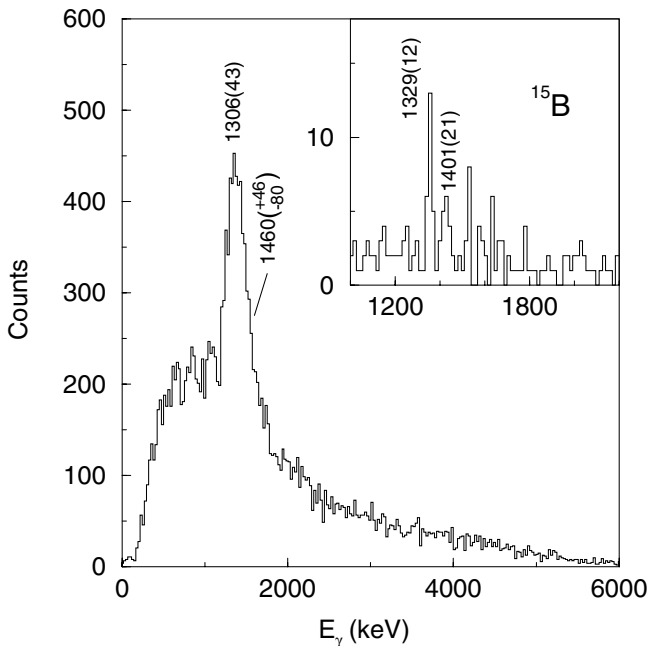


Fig. 2. γ -ray spectrum of ^{15}B by use of BaF_2 detectors. In the insert the same spectrum measured by Ge detectors is shown.

which allows the assumption that these states are the same. In this case, using the energy values given above and the $1/\sigma^2$ weights, the energy of the first-excited state in ^{14}B is 655 ± 5 keV. The two states, in principle, may also be different due to the different excitation mechanisms applied in the two studies, although, no other bound excited state is expected from the *psd* shell model.

The γ -ray spectrum of ^{15}B produced by the BaF_2 detectors is shown in fig. 2. The spectrum measured by the Ge detectors is presented as an inset. In the Ge spectrum of ^{15}B a stronger line is present at 1329 keV and there is an indication for a weaker one at 1401 keV. Due to the low resolution of the BaF_2 detectors, these two lines are seen as a single wide peak in the BaF_2 spectrum. Knowing the width of peaks from the systematics of single peaks of other nuclei, the two lines could be resolved. Their energies were fitted as 1306 ± 43 and 1460_{-80}^{+46} keV, respectively. The uncertainties of the energies come from the uncertainty of the energy calibration (26 keV), the statistical uncertainties of the peak positions (28 and 38 keV, respectively) and a systematic error caused by the possibility of using different shapes for the background below the peak. The energies are especially sensitive to the position where the background is reaching the high-energy tail of the peak. The deviation of the mean energies deduced from the two spectrometers for the higher-energy γ -ray may suggest that the background has been slightly underestimated in the fit, which is expressed via the asymmetric uncertainty of the energy value. The adopted value of the γ -ray energies can be obtained by use of the energy values from both types of detectors and the $1/\sigma^2$ weighting factors (assuming $\sigma = (46 + 80)/2 = 63$ keV for the 1460 keV line) at $E_\gamma = 1327(12)$ and $1407(20)$ keV. It

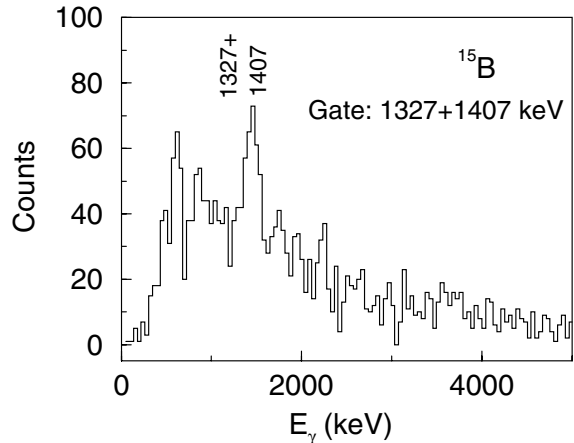


Fig. 3. $\gamma\gamma$ -coincidence spectrum of ^{15}B gated on the 1327 and 1407 keV transitions.

is worth pointing out that the observation of a peak at ~ 1.35 MeV has been reported in two other experiments using in-beam γ -ray spectroscopy with double-step fragmentation reactions [3,4]. Counting statistics of the BaF_2 array was sufficient to extract some information on $\gamma\gamma$ -coincidences. By gating on the 1327 + 1407 keV doublet, it was found that the two lines of the doublet are in coincidence with each other as can be seen in fig. 3. This situation is confirmed also by the coincidence spectra of ref. [3].

As the intensity of the 1327 keV transition is stronger than the 1407 keV one, it is assigned to the decay of the first-excited state to the ground state. The weaker 1407 keV transition is placed on top of the 1327 keV establishing another state at 2734(32) keV excitation energy. This state is situated just below the neutron separation energy of 2770(30) keV [15]. The proposed level scheme together with the results of the theoretical calculations is shown in fig. 4.

The ground-state spin and parity of ^{15}B were determined by Sauvan *et al.* [16] as $3/2^-$ in agreement with the theoretical expectations. All the theories predict a $5/2^-$ spin-parity value for the first-excited state. This state can be assigned to the experimentally observed state at 1327 keV. Among the theoretically predicted low-lying states, the $7/2^-$ one is expected to feed the $5/2^-$ state via an $M1$ transition with higher intensity than a decay to the ground state through an $E2$ transition. On the other hand, the decay of the other possible bound state with spin $1/2$ is expected to feed the ground state with higher intensity via a high-energy $M1$ transition branch, and a lower-energy $E2$ transition to the $5/2$ state would be weaker. Thus, on the basis of its decay properties the level at 2734 keV may be a candidate for the theoretical $7/2^-$ state. Using these tentative assignments, the different theoretical predictions are compared with each other and with the experimental results in fig. 4.

The common point in predictions of the different models is that all of them expect a ground-state band with the spin sequence $3/2^-$, $5/2^-$ and $7/2^-$. This is very likely, due to the coupling of a $p_{3/2}$ proton hole to the 2^+ excited

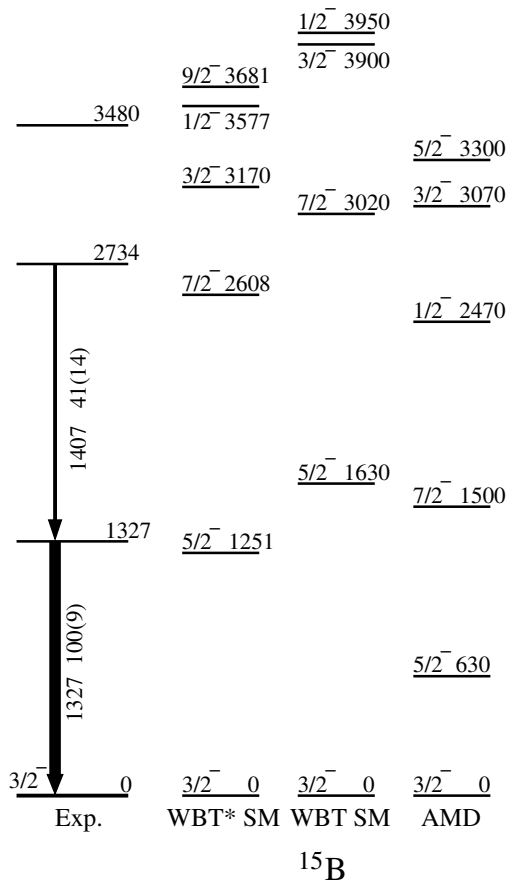


Fig. 4. Proposed level scheme of ^{15}B . Along the transitions their energies and relative intensities with uncertainties are given. The results of the shell and AMD model calculations are included in the right part of the figure. The unbound experimental state at 3480 keV is taken from ref. [2].

state in ^{16}C , which has an almost pure neutron configuration [17]. As a matter of fact, this coupling produces a multiplet of negative-parity states with a spin sequence going from $1/2$ to $7/2$. The shell model calculation using the WBT interaction [7] agrees more with the experimental spectrum than the AMD model. However, the experimental spectrum is compressed by about 10% as compared to shell model theory. A similar feature has also been observed in the $^{16-20}\text{C}$ isotopes [18]. It can be traced back to the weakly bound nature and consequently to the relatively large radii of these nuclei [1], as compared to those for which this interaction was developed. The matrix elements of the two-body interaction are approximately inversely proportional to the squared radius. Therefore, a simple method for compensation of the effects of weak binding is to reduce the two-body matrix elements. In this region, a renormalization of the matrix elements of the sd shell interaction by a factor of 0.75 was appropriate. The renormalized interaction is called the WBT* interaction. Using this modified interaction, the calculated energies of the members of the ground-state band of ^{15}B give a nice agreement with the experiment, as is shown in fig. 4.

Summarizing our results, we have observed bound excited states in ^{15}B for the first time. Comparing the experimental energies with those obtained from shell model calculations it was found that the ground-state band is more compressed than the calculated one, which could be interpreted as a consequence of the weakly bound nature of the valence neutrons in this very neutron-rich nucleus ($A/Z = 3$).

The experiment using in-beam γ spectroscopy with fragmentation reactions benefits from the availability of ^{36}S isotope kindly provided by our colleagues from DUBNA, and from the smooth running of the accelerator by the GANIL crew. This work has been supported by the European Community contract No. HPRI-CT-1999-00019, and also from OTKA T38404, T42733, T46901, PICS(IN2P3) 1171, INTAS 00-00463, RFBR N96-02-17381a, GA ASCR A 1048 102, and NSF PHY-0244453 grants, as well as from Bolyai János Foundation.

References

1. I. Tanihata, T. Kobayashi, O. Yamakawa, S. Shimoura, K. Ekuni, K. Sugimoto, N. Takahashi, T. Shimoda, H. Sato, Phys. Lett. B **206**, 592 (1988).
2. R. Kalpakchieva, H.G. Bohlen, W. von Oertzen, B. Gebauer, M. von Lucke-Petsch, T.N. Massey, A.N. Ostrowski, Th. Stolla, M. Wilpert, Th. Wilpert, Eur. Phys. J. A **7**, 451 (2000).
3. M. Stanoiu, PhD Thesis, GANIL T 03 01 (Ganil, Caen, 2003).
4. Y. Kondo *et al.*, RIKEN Accelerator Progress Report 2002 (Riken, Wako, 2003) p. 65.
5. Y. Kanada-Enyo, H. Horiuchi, Phys. Rev. C **52**, 647 (1995).
6. N.A.F.M. Poppelier, L.D. Wood, P.W.M. Glaudemans, Phys. Lett. B **157**, 120 (1985).
7. E.K. Warburton, B.A. Brown, Phys. Rev. C **46**, 923 (1992).
8. M.-J. Lopez-Jimenez, PhD Thesis, GANIL T 00 01 (Ganil, Caen, 2000); *International Winter Meeting on Nuclear Physics, Bormio 1999*, Ric. Sci. Educ. Perm., Suppl. **114**, 416 (1999).
9. M. Belleguic-Pigeard de Gurbert, PhD Thesis, IPNO-T-00-05 (Institute de Physique Nucleaire, Orsay, 2000); M. Belleguic *et al.*, Nucl. Phys. A **682**, 136c (2001).
10. Zs. Dombrádi *et al.*, Nucl. Phys. A **727**, 195 (2003).
11. O. Sorlin *et al.*, *Structure of the neutron-rich $^{37,39}\text{P}$ and $^{43,45}\text{Cl}$ nuclei*, to be published in Eur. Phys. J. A.
12. D. Sohler *et al.*, Phys. Rev. C **66**, 054302 (2002).
13. M. Stanoiu *et al.*, Phys. Rev. C **69**, 034312 (2004).
14. F. Ajzenberg-Selove, J.H. Kelley, C.D. Nesaraja, Nucl. Phys. A **523**, 1 (1991).
15. M.A.C. Hotchkis, L.K. Fifield, J.R. Leigh, T.R. Ophel, G.D. Putt, D.C. Weisser, Nucl. Phys. A **398**, 130 (1983).
16. E. Sauvan *et al.*, Phys. Lett. B **491**, 1 (2000).
17. Z. Elekes *et al.*, Phys. Lett. B **586**, 34 (2004).
18. O. Sorlin *et al.*, *Proceedings of the International Conference on the Labyrinth in Nuclear Structure, 13-19th July 2003, Crete*, edited by A. Bracco, C.A. Kalfas, AIP Conf. Proc. **701**, 31 (2004).